5-30-2007

Albumin-binding PARACEST Agents

M. Meser Ali
University of Texas at Dallas

Mark Woods
Portland State University, mark.woods@pdx.edu

Eul Hyun Suh
University of Texas Southwestern Medical Center

Zoltan Kovacs
University of Texas Southwestern Medical Center

Gyula Tircsó
University of Texas at Dallas

See next page for additional authors

Citation Details

Ali, M. M., Woods, M., Suh, E. H., Kovacs, Z., Tircsó, G., Zhao, P., ... & Sherry, A. D. (2007). Albumin-binding PARACEST agents. JBIC Journal of Biological Inorganic Chemistry, 12(6), 855-865.

Published in final edited form as:
J Biol Inorg Chem. 2007 August ; 12(6): 855–865. doi:10.1007/s00775-007-0240-z.

Albumin-binding PARACEST agents

M. Meser Ali,
Department of Chemistry, University of Texas at Dallas, P.O. Box 830688, Richardson, TX 75083-0688, USA

Mark Woods,
Department of Chemistry, University of Texas at Dallas, P.O. Box 830688, Richardson, TX 75083-0688, USA

Macrocyclics, Inc, 2110 Research Row, Suite 425, Dallas, TX 75235, USA

Eul Hyun Suh,
Advanced Imaging Research Center, University of Texas Southwestern Medical Center, 2201 Inwood Road, Dallas, TX 75390-8568, USA, e-mail: dean.sherry@utsouthwestern.edu

Zoltan Kovacs,
Advanced Imaging Research Center, University of Texas Southwestern Medical Center, 2201 Inwood Road, Dallas, TX 75390-8568, USA, e-mail: dean.sherry@utsouthwestern.edu

Gyula Tircsó,
Department of Chemistry, University of Texas at Dallas, P.O. Box 830688, Richardson, TX 75083-0688, USA

Piyu Zhao,
Department of Chemistry, University of Texas at Dallas, P.O. Box 830688, Richardson, TX 75083-0688, USA

Vikram D. Kodibagkar, and
Department of Radiology, University of Texas Southwestern Medical Center, 5323 Harry Hines Blvd, Dallas, TX 75390, USA

A. Dean Sherry
Department of Chemistry, University of Texas at Dallas, P.O. Box 830688, Richardson, TX 75083-0688, USA

Advanced Imaging Research Center, University of Texas Southwestern Medical Center, 2201 Inwood Road, Dallas, TX 75390-8568, USA, e-mail: dean.sherry@utsouthwestern.edu

Abstract

Lanthanide complexes (Eu^{3+}, Gd^{3+} and Yb^{3+}) of two different 1,4,7,10-tetraazacyclododecane-1,4,7,10-tetraacetic acid tetraamide derivatives containing two (**2**) and four (**3**) *O*-benzyl-L-serine amide substituents were synthesized and their chemical exchange saturation transfer (CEST) and relaxometric properties were examined in the presence and absence of human serum albumin (HSA). Both Eu**2** and Eu**3** display a significant CEST effect from a single slowly exchanging Eu^{3+}-bound water molecule, making these PARACEST complexes potentially useful as vascular MRI agents. Yb**2** also showed a detectable CEST effect from both the Yb^{3+}-bound water protons and the exchangeable NH amide protons, making it potentially useful as a vascular pH sensor. Fluorescence displacement studies using reporter molecules indicate that both Gd**2** and Gd**3** displace

Correspondence to: A. Dean Sherry.

dansylsarcosine from site II of HSA with inhibition constants of 32 and 96 μM, respectively, but neither complex significantly displaces warfarin from site I. Water proton relaxation enhancements of 135 and 171% were observed upon binding of Gd**2** and Gd**3** to HSA, respectively, at 298 K and pH 7.4.

Keywords

Chemical exchange saturation transfer agents; MRI contrast; Albumin binding; Paramagnetic relaxation

Introduction

Magnetic resonance imaging (MRI) is one of the most powerful and versatile tools in biomedicine, providing not only high-resolution anatomical images but also functional data such as blood flow, tissue perfusion, and distribution of metabolites. MRI detects mostly tissue water and fat and does not require injection of exogenous agents to produce image contrast. Nevertheless, paramagnetic contrast agents (CAs) are often used to selectively alter tissue contrast by altering the relaxation rate of tissue water. Current diagnostic CAs for MRI are largely based on paramagnetic gadolinium complexes [1,2] that highlight only those tissue regions where an agent accumulates for a period of time that is abnormal compared with that for well-vascularized tissue. Accumulation of a Gd^{3+}-based agent results in a shortening of the bulk water spin-lattice relaxation time (T_1) and hence brightening of the image in that region. Although current nonspecific, extracellular Gd^{3+}-based agents are widely accepted and used clinically, interest in “smart” or “responsive” agents that can provide additional physiological or metabolic information to aid in a clinical diagnosis is growing.

Recently a new class of CA based upon a chemical exchange saturation transfer (CEST) mechanism have been proposed and demonstrated. Unlike other image-darkening agents that function by shortening the transverse relaxation time (T_2) of water protons, CEST agents act by decreasing the water signal intensity via chemical exchange of saturated spins. This approach was first demonstrated by Ward and Balaban [3] using low molecular weight diamagnetic molecules containing exchangeable OH or NH groups. They showed that magnetic resonance contrast can be switched on/off by applying a saturating irradiation pulse and, since chemical exchange between such groups and bulk water is pH dependent, such systems can potentially be used to image tissue pH [3,4]. One disadvantage of such diamagnetic agents is that the chemical shift difference between exchanging OH and NH protons and bulk water is typically quite small, often less than 5 ppm. This makes it difficult to selectively activate the CEST agent in tissues where the bulk water signal can be rather broad. Nevertheless, Geoffeney et al. [5], Snoussi et al. [6], and Zhou et al. [7] have shown that CEST can be amplified by using endogenous and exogenous macromolecules with large numbers of exchanging sites or endogenous proteins or peptides. We recently reported that the weakly paramagnetic Eu**1** (Structure 1) has a Eu^{3+}-bound water resonance near 50 ppm that can be used as an RF antenna to initiate CEST. Protons on this bound water molecule also have a much shorter exchange lifetime ($\tau_M^{298}=350\,\mu s$) compared with diamagnetic NH or OH protons, a feature that can potentially enhance CEST contrast at equivalent agent concentrations [8,9]. Since that early report, several other papers have appeared on responsive paramagnetic CEST agents capable of sensing physiological indices such as pH [10–12], lactate [13], glucose [14], and temperature [4,15].

Just as one might amplify the effect of a Gd^{3+}-based T_1 agent by conjugation to a higher molecular weight macromolecule such as albumin, polylysine, or a dendrimer, one could also conjugate multiple PARACEST agents to a polymer backbone to decrease the “effective”

concentration of the agent. Since the CEST efficiency of such agents is highly dependent upon the rate of water exchange, one question of interest is whether interactions between a PARACEST agent and protein surface residues for example might either enhance or quench the CEST effect. To test this hypothesis, we prepared and characterized PARACEST agents containing two (Ln**2**) or four (Ln**3**) *O*-benzyl functionalities, groups known to impart a high binding affinity for albumin [16,17] (Structure 1). The albumin-binding properties of these agents were measured using fluorescence spectroscopy and their CEST behavior in the presence and absence of albumin was measured to determine whether water or proton exchange was altered upon binding of the agent to albumin.

Materials and methods

General remarks

All reagents and solvents were purchased from commercially available sources and used as received. ^{1}H, CEST and ^{13}C spectra were recorded with a JEOL Eclipse 270 spectrometer or a Varian INOVA-400 spectrometer operating at 270 and 67.5 MHz or 400 and 100 MHz, respectively. Water proton relaxation measurements were made using an inversion-recovery pulse sequence with a MRS-6 NMR analyzer (Institut "Jožef Stefan," Ljubljana, Slovenia) operating at 20 MHz. IR spectra were recorded using a PerkinElmer 1600 Fourier transform IR spectrophotometer. Melting points were determined with a Fisher–Johns melting point apparatus and are uncorrected.

1,7-Dibenzyloxycarbonyl-1,4,7,10-tetraazacyclododecane was prepared according to previously published methods [18].

2-(2-Bromoacetamido)-3-(benzyloxy)propanoic acid

A solution of bromoacetyl bromide (12.9 g; 64.0 mmol) in CH_2Cl_2 (20 mL) was added dropwise to a solution of 2-amino-3-(benzyloxy)propanoic acid (5.0 g, 25.6 mmol) and potassium carbonate (14.2 g, 102.4 mmol) in aqueous 2 N NaOH (12 mL) at 273 K. The reaction mixture was stirred at 273 K for 10 min before warming it to room temperature and stirring for a further 2 h. The two layers were separated, and the pH of the aqueous layer was adjusted to between 1 and 2 with 20% hydrochloric acid. The aqueous phase was then extracted with CH_2Cl_2 (200 mL). The organic extracts were washed with water (2 × 100 mL), dried (Na_2SO_4), and the solvents were removed under reduced pressure to afford 2-(2-bromoacetamido)-3-(benzyloxy)propanoic acid (**4**) as a colorless gum (5.70 g, 70%). ^{1}H NMR (400 MHz, $CDCl_3$, δ): 10.38 (1H, s br, COOH), 7.26 (5H, m, Ar), 4.68 (1H, m, NC<u>H</u>CO), 4.53 (1H, d aa′ system, $^{2}J_{H–H}$ = 12 Hz, OC<u>H</u>$_2$Ar), 4.47 (1H, d aa′ system, $^{2}J_{H–H}$ = 12 Hz,OC<u>H</u>$_2$Ar), 4.04–3.44 (4H, m, CHC<u>H</u>$_2$O, COC<u>H</u>$_2$Br). ^{13}C NMR (100 MHz, $CDCl_3$, δ): 173.6 (N<u>C</u>O$_2$), 166.9 (NHC=O), 137.3 (<u>Ar</u>), 128.8 (Ar), 128.3 (Ar), 128.0 (Ar), 73.6 (O<u>C</u>H$_2$Ar), 69.1 (CH<u>C</u>H$_2$O), 53.5 (<u>C</u>H), 28.7 (CO<u>C</u>H$_2$Br); ν_{max} (cm^{-1}): 3,379 (br, OH), 2,969, 2,938, 2,866, 1,733 (C=O); 1,652 (C=O), 1,538, 1,454, 1,396, 1,361, 1,206, 1,105, 1,048. *m/z* (ESMS, ESI–): 316 (100%, $[M – H]^-$); an appropriate bromine isotope pattern was observed.

tert-Butyl 2-(2-bromoacetamido)-3-(benzyloxy)propanoate

To a solution of the acid **4** (5.5 g, 17.5 mmol) in tetrahydrofuran (THF; 150 mL) cooled in an ice bath was slowly added *tert*-butyl trichloroacetimidate (9.6 g, 43.8 mmol) in THF (50 mL). After addition was complete, $BF_3{\cdot}OEt_2$ (0.66 mL, 5.3 mmol) was also added very slowly. The reaction mixture was allowed to warm to room temperature and stirred for 12 h. The resulting solution was diluted with diethyl ether (200 mL) and washed with saturated aqueous $NaHCO_3$ (2 × 60 mL), water (2 × 80 mL), and dried (Na_2SO_4). The solvents were removed in vacuo and the residue suspended in CH_2Cl_2 (30 mL). The suspension was cooled to 273 K and allowed to stand for 1 h. The solids were removed by filtration and the solvents were removed

in vacuo. The oily residue was purified by column chromatography over silica gel eluting with 5% CH_3OH in CH_2Cl_2 to afford *tert*-butyl 2-(2-bromoacetamido)-3-(benzyloxy)propanoate (**5**) as a colorless oil (3.7 g, 56%). R_f = 0.71 (SiO_2, 5% CH_3 OH in CH_2Cl_2). ^{1}H NMR (400 MHz, $CDCl_3$, δ): 7.25 (5H, m, Ar), 4.54 (1H, m, NHC<u>H</u>CH_2), 4.51 (1H, d aa′ system, $^2J_{H–H}$ = 12 Hz, OC<u>H</u>$_2$Ar), 4.44 (1H, d aa′ system, $^2J_{H–H}$ = 12 Hz, OC<u>H</u>$_2$Ar), 3.90–3.47 (4H, m, CHC<u>H</u>$_2$O, COCH_2Br), 1.41 (9H, s, C(C<u>H</u>$_3$)$_3$). ^{13}C NMR (100 MHz, $CDCl_3$, δ): 169.2 (CO_2), 166.1 (NHC=O), 138.1 (Ar), 129.0 (Ar), 128.4 (Ar), 128.3 (Ar), 83.2 [<u>C</u>(CH_3)$_3$], 73.9 (O<u>C</u>H$_2$Ar), 70.2 (CH<u>C</u>H$_2$O), 54.4 (NH<u>C</u>HCH$_2$), 29.4 (CO<u>C</u>H$_2$Br), 28.6 [C(<u>C</u>H$_3$)$_3$]. ν_{max} (cm^{-1}): 2,974, 2,920, 2,862, 1,734 (C=O), 1,652 (C=O), 1,539, 1,520, 1,506, 1,455, 1,393, 1,367, 1,242, 1,149, 1,104, 1,032. *m/z* (ESMS, ESI–): 370 (100%, $[M – H]^-$); an appropriate bromine isotope pattern was observed.

1,4,7,10-Tetraazacyclododecane-1,4,7,10-tetra-(2-(methylene benzyloxy ether)-*tert*-butyl acetate) acetamide

The bromoacetamide **5** (1.4 g, 4.1 mmol), cyclen (170 mg, 0.96 mmol), and *N*,*N*-diisopropylethylamine (0.9 g, 7.0 mmol) were dissolved in CH_3CN (30 mL). The resulting solution was heated with stirring at 328 K for 3 days. The reaction mixture was then cooled to room temperature and the solvents removed in vacuo. The oily residue was taken up in $CHCl_3$ (200 mL) and washed with water (2 × 75 mL). The organic layer was dried (Na_2SO_4) and solvents were removed under reduced pressure. The oily residue was then titrated with diethyl ether to afford 1,4,7,10-tetraazacyclododecane-1,4,7,10-tetra-(2-(methylene benzyloxy ether)-*tert*-butyl acetate) acetamide (**6**) as a colorless gum (1.1 g, 93%). ^{1}H NMR (270 MHz, $CDCl_3$, δ): 7.25 (24H, m, Ar and NH), 4.65 (4H, m, CH), 4.54 (4H, q aa′ system, $^2J_{H–H}$ = 12 Hz, C<u>H</u>$_2$Ar), 4.52 (4H, q aa′ system, $^2J_{H–H}$ = 12 Hz, C<u>H</u>$_2$Ar), 3.85 (8H, m, CH<u>C</u>H$_2$), 3.70 (8H, s br, N<u>C</u>H$_2$CO), 3.50-2.80 (16H, m br, NCH_2 ring), 1.20 [36H, s, C(C<u>H</u>$_3$)]. ^{13}C NMR (68 MHz, $CDCl_3$, δ): 170.0 (C=O), 169.2 (C=O), 137.7 (Ar), 128.5 (Ar), 128.0 (Ar), 127.9 (Ar), 73.31 [<u>C</u>(CH_3)$_3$], 69.2, (O<u>C</u>H$_2$Ar), 57.1 (CH<u>C</u>H$_2$), 53.0 (NCH_2 ring), 52.2 (CH), 51.1 (NCH_2O), 14.2 [C(<u>C</u>H$_3$)$_3$]. *m/z* (ESMS ESI+): 1,224 (100%, $[M + H]^+$).

1,4,7,10-Tetraazacyclododecane-1,4,7,10-tetra-[2-(methylene benzyloxy ether)-acetic acid] acetamide

The *tert*-butyl ester **6** (1.0 g, 0.72 mmol) was dissolved in 50% trifluoroacetic acid (TFA) in CH_2Cl_2 (10 mL). The resulting solution was stirred at room temperature for 5 h. The solvents were removed under vacuum and dichloromethane (20 mL) was added to the residue. The solvents were again removed under reduced pressure and this procedure was repeated a total of three times. After drying under high vacuum, 1,4,7,10-tetraazacyclododecane-1,4,7,10-tetra-[2-(methylene benzyloxy ether)-acetic acid] acetamide (**3**) was obtained as a colorless gum (0.55 g, 69%). ^{1}H NMR (270 MHz, CD_3OD, δ): 7.28 (5H, m, Ar), 4.63 (4H, m, CH), 4.59 (4H, q aa′ system, $^2J_{H–H}$ = 12 Hz, C<u>H</u>$_2$Ar), 4.47 (4H, q aa′ system, $^2J_{H–H}$ = 12 Hz, C*H*$_2$Ar), 3.82 (8H, m, CHC<u>H</u>$_2$), 3.72 (8H, s, OCH_2N), 3.32-3.21 (16H, m br, NCH_2 ring). ^{13}C NMR (68 MHz, CD_3OD, δ): 172.0 (C=O), 169.2 (C=O), 137.9 (Ar), 128.2 (Ar), 127.8 (Ar), 127.7 (Ar), 73.0 (<u>C</u>HCH$_2$), 69.4 (O<u>C</u>H$_2$Ar), 53.3 (CH_2 ring), 50.8 (CH<u>C</u>H$_2$), 50.7 (NCH_2CO). *m/z* (ESMS, ESI+): 1,113 (100% $[M + H]^+$), 1,135 (20% $[M + Na]^+$).

tert-Butyl 2-(2-chloroacetamido)acetate

Glycine *tert*-butyl ester hydrochloride (6.3 g, 37.8 mmol) and potassium carbonate (15.7 g, 113.5 mmol) were dissolved in water (200 mL) and CH_2Cl_2 (200 mL) was added. The biphasic reaction mixture was cooled to 273 K and a solution of chloroacetyl chloride (8.5 g, 75.6 mmol) in CH_2Cl_2 (40 mL) was added dropwise. The reaction was stirred at 273 K for 30 min and then allowed to warm to room temperature and was stirred for 1 h. The two layers were separated and the organic layer was washed with 5% aqueous citric acid (2 × 40 mL) and water (2 × 40

mL) before drying (Na_2SO_4). The solvents were removed in vacuo to afford *tert*-butyl 2-(2-chloroacetamido)acetate (**7**) as a colorless solid (7.8 g, 99%). Melting point 340.5-341 K. ^{1}H NMR (400 MHz, $CDCl_3$, δ): 7.17 (1H, s br, NH), 4.11 (2H, s, CH_2Cl), 4.00 (2H, d, $^2J_{H–H}$ = 4.0 Hz, NHC$\underline{H}_2$), 1.51 [9H, s, C(C$\underline{H}_3$)$_3$]. ^{13}C NMR (100 MHz, $CDCl_3$, δ): 168.2 (CO_2), 166.0 (NHCO), 82.5 [$\underline{C}(CH_3)_3$], 42.2 (NH$\underline{C}H_2CO$), 42.0 ($ClCH_2$), 27.8 [C($\underline{C}H_3$)$_3$]. ν_{max} (cm^{-1}): 3,245 (NH), 3,087, 2,975, 1,734 (C=O), 1,652 (C=O), 1,557, 1,540, 1,409, 1,365, 1,228, 1,160, 1,039. *m/z* (ESMS, ESI–): 206 (100%, [M – H]$^-$); an appropriate chlorine isotope pattern was observed. Anal. Found (Calcd for $C_8H_{14}ClNO_3$): C, 46.1 (46.3); H, 6.8 (6.8); N, 6.7 (6.8).

1,7-Bis(benzyloxycarbonyl)-4,10-bis(*tert*-butylacetamidoacetate)-1,4,7,10-tetraazacyclododecane

The chloroacetamide **7** (3.0 g, 14.4 mmol) and potassium carbonate (3.0 g, 21.7 mmol) were added to a solution of the diprotected cyclen **8** (3.2 g, 7.2 mmol) in CH_3CN (80 mL). The reaction mixture was heated with stirring at 333 K for 3 days. After cooling to room temperature, the reaction mixture was filtered and the solvents were removed under reduced pressure. The oily residue was dissolved in diethyl ether (200 mL) and washed with water (2 × 50 mL), and dried (Na_2SO_4). The solvents were removed under vacuum and the oily residue was purified by column chromatography over silica gel eluting with 5% CH_3OH and 0.3% NH_4OH in CH_2Cl_2 to afford 1,7-bis (benzyloxycarbonyl)-4,10-bis(*tert*-butyl-acetamidoacetate)-1,4,7,10-tetraazacyclododecane (**9**) as a colorless solid (4.1 g, 73%). R_f = 0.33 (SiO_2, 5% CH_3OH, and 0.3% NH_4OH in CH_2Cl_2). Melting point 334-335.5 K. ^{1}H NMR (270 MHz, $CDCl_3$, δ): 7.29 (10H, m, Ar), 5.06 (4H, s, OCH_2Ar), 3.78 (4H, s br, NHC$\underline{H}_2$CO), 3.42 (8H, s br, NCH_2 ring), 3.17 (4H, s br, NCH_2CO), 2.80 (8H, s br, NCH_2 ring), 1.40 [18H, s, C(CH_3)$_3$]. ^{13}C NMR (68 MHz, $CDCl_3$, δ): 171.3 (NHC=O), 168.9 (NCO_2), 156.9 (NHC=O), 136.6 (Ar), 128.6 (Ar), 128.4 (Ar), 128.3 (Ar), 81.8 [$\underline{C}(CH_3)_3$], 67.4 (O$\underline{C}H_2Ar$), 58.4 (NCH_2 ring), 55.1 (N$\underline{C}H_2CO$), 48.9 (NCH_2 ring), 41.6 (NH$\underline{C}H_2CO$), 28.1 (C($\underline{C}H_3$)$_3$). ν_{max} (cm^{-1}): 3,288 (NH), 2,974, 2,922, 2,811, 1,740 (C=O), 1,687 (C=O), 1,650 (C=O), 1,521, 1,456, 1,416, 1,366, 1,220, 1,151. *m/z* (MALDI/TOF): 783 (100% [M + H]$^+$). Anal. Found (Calcd for $C_{40}H_{58}N_6O_{10}$·0.2HCl): C, 60.6 (60.8); H, 7.3 (7.4); N, 10.4 (10.6).

1,7-Bis(*tert*-butyl acetamidoacetate)-1,4,7, 10-tetraazacyclododecane

To a solution of the dicarbamate **9** (8.2 g, 10.5 mmol) in absolute ethanol (80 mL) was added 10% Pd on carbon (1.0 g). The mixture was placed on a Parr hydrogenation apparatus and shaken under a hydrogen pressure of 40 psi for 3 days. The reaction mixture was then filtered and the solvents were removed from the filtrate under reduced pressure toafford 1,7-bis(*tert*-butyl acetamidoacetate)-1,4,7,10-tetraazacyclododecane (**10**) as a colorless oil (5.2 g, 96%). ^{1}H NMR (270 MHz, $CDCl_3$, δ): 7.77 (2H, s br, NH), 3.83 (4H, d, $^2J_{H–H}$ = 4 Hz, NHC$\underline{H}_2$CO), 3.17 (4H, s, NCH_2CO), 2.69-2.64 (16H, m br, NCH_2 ring), 1.30 [18H, s, C(CH_3)$_3$]. ^{13}C NMR (68 MHz, $CDCl_3$, δ): 171.6 (CO_2), 169.6 (CONH), 82.0 [$\underline{C}(CH_3)_3$], 60.5 (NH$\underline{C}H_2CO$), 53.0 (NCH_2 ring), 46.5 (NCH_2 ring), 41.7 (N$\underline{C}H_2CO$), 28.1 [C($\underline{C}H_3$)$_3$] ν_{max} (cm^{-1}): 3,288 (NH), 2,974, 2,915, 1,740 (C=O), 1,689 (C=O), 1,524, 1,454, 1,416, 1,366, 1,263, 1,152, 730. *m/z* (MALDI/TOF): 515 (100% [M + H]$^+$).

1,7-Bis[2-(methylene benzyloxy ether)-*tert*-butyl acetate] acetamide-4,10-bis(*tert*-butylacetamidoacetate)-1,4,7,10-tetraazacyclododecane

Hünig's base (3.53 g, 27.30 mmol) and the bromoacetamide **5** (3.4 g, 9.1 mmol) were added to a solution of the diamide **10** (2.3 g, 4.6 mmol) in CH_3CN (60 mL). The reaction mixture was heated with stirring at 333 K for 3 days. After cooling to room temperature, the solvents were removed under reduced pressure and the oily residue was taken up into diethyl ether (150 mL). The solution was filtered and the solvents were removed from the filtrate to afford 1,7-bis[2-(methylene benzyloxy ether)-*tert*-butyl acetate] acetamide-4,10-bis(*tert*-butyl-

acetamidoacetate)-1,4,7,10-tetraazacyclododecane (**11**) as a glassy solid, which was used for the next step without further purification. Melting point 330-333 K. ^{1}H NMR (400 MHz, $CDCl_3$, δ): 8.32 (2H, s br, NH), 7.45 (2H, s br, NH), 7.18 (10H, m, Ar), 4.49 (2H, m, NC$\underline{H}CO_2$), 4.44 (2H, d aa′ system, $^2J_{H–H}$ = 12 Hz, OCH_2Ar), 4.36 (2H, d aa′ system, $^2J_{H–H}$ = 12 Hz, OCH_2Ar), 3.77 (8H, m, $CHC\underline{H}_2O$, $NC\underline{H}_2CO_2$), 3.65 (4H, s br, $NC\underline{H}_2CO$), 3.43 (4H, s br, $NC\underline{H}_2CO$), 2.45–3.20 (16H, br, NCH_2 ring), 1.34 [18H, s, $C(CH_3)_3$], 1.32 [18H, s, $C(CH_3)_3$]. ^{13}C NMR (100 MHz, $CDCl_3$, δ): 193.2 (CO_2), 188.0 (CO_2), 169.6 (NHC=O), 169.4 (NHC=O), 138.0 (Ar), 129.0 (Ar), 128.4 (Ar), 128.3 (Ar), 82.9 [$\underline{C}(CH_3)_3$], 73.9 ($O\underline{C}H_2Ar$), 70.3 ($CH\underline{C}H_2O$), 62.5 ($N\underline{C}HCH_2$), 57.1 ($N\underline{C}H_2CO$), 53.7 (br, NCH_2 ring), 42.3 ($N\underline{C}H_2CO_2$), 28.6 [$C(\underline{C}H_3)_3$], 28.5 [$C(\underline{C}H_3)_3$]. ν_{max} (cm^{-1}): 2,974, 2,922, 2,828, 2,812, 1,739 (C=O), 1,670 (C=O), 1,517, 1,454, 1,392, 1,366, 1,222, 1,152, 1,104. *m/z* (MALDI/TOF): 1,097 (100%, [M + H^+]).

1,7-Bis[2-(methylene benzyloxy ether)-acetic acid] acetamide-4,10-bis(acetamidoacetic acid)-1,4,7,10-tetraazacyclododecane

The *tert*-butyl ester **11** (1.0 g; 0.9 mmol) was dissolved in CH_2Cl_2 (5 mL) and TFA (8 mL) was added. The reaction mixture was stirred at 298 K for 12 h and the solvents were removed under reduced pressure. The resulting oily residue was washed with diethyl ether (3 × 50 mL) and dried under vacuum. The solid residue was dissolved in water (18 mL) and purified by preparative reversed-phase high-performance liquid chromatography (HPLC) over a Phenomenex Luna C-18(2) (250 mm × 50 mm) column on a Waters δ-prep HPLC system. Absorbance was monitored at 205 and 254 nm. The system was eluted with water (0.1% TFA) for 5 min and then with a linear gradient to 50% MeCN (0.1% TFA) and 50% water (0.1% TFA) after 15 min and maintained isocratically for a further 10 min, at a flow rate of 100 mL min^{-1}. 1,7-Bis[2-(methylene benzyloxy ether)-acetic acid] acetamide-4,10-bis (acetamidoacetic acid)-1,4,7,10-tetraazacyclododecane (**2**) was obtained as a colorless solid (0.44 g, 68%). HPLC R_t = 17.8 min. Melting point 397-399 K. ^{1}H NMR (400 MHz, ND_3OD, δ): 7.15 (10H, m, Ar), 4.39 (2H, m, NC$\underline{H}CO_2$), 4.38 (2H, d aa′ system, $^2J_{H–H}$ = 12 Hz, OCH_2Ar), 4.32 (2H, d aa′ system, $^2J_{H–H}$ = 12 Hz, OCH_2Ar), 4.11–3.34 (16H, m, $CHC\underline{H}_2O$, $NC\underline{H}_2CO_2$, $NC\underline{H}_2CO$), 2.40–3.34 (16H, m br, NCH_2 ring). ^{13}C NMR (100 MHz, $CDCl_3$, δ): 172.9 (CO_2), 163.2 (NHC=O), 162.8 (NHC=O), 137.1 (Ar), 128.8 (Ar), 128.5 (Ar), 128.4 (Ar), 73.0 ($O\underline{C}H_2Ar$), 68.5 ($CH\underline{C}H_2O$], 55.1 ($N\underline{C}H_2CO$), 54.5 ($N\underline{C}HCH_2$), 53.2 ($N\underline{C}H_2CO$), 50.0 (br, NCH_2 ring), 41.1 ($N\underline{C}H_2CO_2$). ν_{max} (cm^{-1}): 3,318 (OH), 2,973, 2,839, 1,731 (C=O), 1,688 (C=O), 1,538, 1,505, 1,455, 1,194, 1,134. *m/z* (MALDI/TOF): 873 (100% [M + $H]^+$). Anal. Found (Calcd for $C_{40}H_{56}N_8O_{14}·3CF_3CO_2H·H_2O$): C, 45.3 (44.8); H, 4.9 (5.0); N, 9.0 (9.1).

General procedure for the preparation of lanthanide(III) complexes

An aqueous lanthanide chloride solution (0.21 M, 614 μL) was added to a solution of ligand **3** (0.14 g, 0.13 mmol) in 50:50 water/methanol (15 mL, pH 6.0). The resulting solution was stirred for 3 days at 333 K and the pH was maintained between 6 and 7 throughout by addition of 1 N KOH. The absence of free Ln^{3+} (Eu or Gd) was verified by colorimetric assay using xylenol orange (1 M AcONa/AcOH buffer, pH 5.3). The reaction mixture was allowed to cool to room temperature and the solvents were removed by freeze-drying. Eu**2** *m/z* (ESMS, ESI +): 1,022 (100% [M – 2H]$^+$); an appropriate isotope pattern was observed. Gd**2** *m/z* (ESMS, ESI+): 1,030 (100% [M – 2H]$^+$); an appropriate isotope pattern was observed. Yb**2** *m/z* (ESMS, ESI+): 1,044 (100% [M – 2H]$^+$); an appropriate isotope pattern was observed. Eu**3**: *m/z* (ESMS, ESI+): 1,263 (100%, [M – 2H]$^+$); an appropriate isotope pattern was observed. Gd**3** *m/z* (ESMS, ESI+): 632 (100% [M – H]$^{2+}$); an appropriate isotope pattern was observed.

CEST measurements

A quantitative description of the NMR behavior of two or more exchanging pools of nuclei is described by the Bloch equations modified for exchange [19]. For the simplest situation of two exchanging pools A and B, it has been shown that the maximum reduction in the water signal intensity (M_Z^a/M_0^a) occurs when (1) the nuclei in pool B are completely saturated so that $M_Z^b=0$ and (2) there is no direct excitation of pool A nuclei by the $\boldsymbol{B}_1$ irradiation that excites B nuclei. Condition 1 is met when $\boldsymbol{B}_1$ is sufficiently large. Condition 2 is met when the relative difference in resonance frequency of the two pools ($\Delta\omega$) is very large so that $\Delta\omega/\omega_1 \gg 1$. Under these conditions, the steady-state solution of the Bloch equations gives

$$\frac{M_Z^a}{M_0^a}=\frac{\tau_a}{\tau_a+T_{1a}}=\frac{1}{1+\frac{cq}{55.5}\frac{T_{1a}}{\tau_M}}, \quad (1)$$

where c is the concentration of the PARACEST agent and q is the number of bound water molecules per PARACEST complex; τ_a is the residence lifetime in pool A, which is related, through the relative concentration of the two pools, to τ_M, the residence lifetime in pool B; and T_{1a} is spinlattice relaxation time of bulk water.

CEST images were acquired using a 200-MHz (^{1}H) Varian Inova scanner. Spin-echo images of two phantoms each containing 20 mM solutions of Eu**2**, one with and one without 5% albumin, were acquired using a 6-s presaturation pulse applied off-resonance (−54 ppm) and on-resonance (54 ppm), respectively, for each phantom. The percentage CEST enhancement map, E, was computed from these images, where $E = 100 \times (S_{off} - S_{on})/S_{off}$, using MATLAB image processing software.

Results and discussion

Synthesis

The synthetic routes to ligands **2** and **3** are outlined in Scheme 1. *O*-Benzyl-L-serine was neutralized with sodium hydroxide and reacted with bromoacetyl bromide in a biphasic reaction using potassium carbonate as a base. The carboxylate of the resulting bromoacetamide **4** was protected as a *tert*-butyl ester using *tert*-butyl trichloroace-timidate and BF_3·OEt. Although the yields for preparing derivatives of 1,4,7,10-tetraazacyclododecane-1,4,7,10-tetraacetic acid (DOTA) where the *O*-benzyl substituent is in the α-position of the acetate side arms was reportedly low [20,21], alkylation of cyclen with 4 equiv of **5** in acetonitrile using Hünig's base at 328 K afforded the protected ligand **6** in 93% yield. Ligand **6** was then deprotected using TFA to afford **3** in 25% overall yield from *O*-benzyl serine.

The *trans*-*O*-benzyl serine substituted ligand **2** was prepared by first preparing bisbenzylcarbamate-protected cyclen from a well-established procedure using benzyl chloroformate [18]. The *tert*-butyl ester of glycine was reacted with chloroacetyl chloride in a biphasic reaction using potassium carbonate as a base to afford the chloroacetamide **7**. This was reacted with **8** using standard alkylating conditions to give **9** and the carbamate protecting groups were then removed by catalytic hydrogenolysis over palladium on carbon to afford the bisamide **10** in 96% yield. **10** was then alkylated with **5** in acetonitrile using Hünig's base to give the tetra-*tert*-butyl ester **11**. Subsequent deprotection using TFA afforded **2** in 48% overall yield from compound **8**.

Lanthanide complexes of **2** and **3** were prepared by mixing equimolar quantities of the ligand and the appropriate lanthanide chloride in a water/methanol solution at 333 K. The isolated

yields of the complexes of **3** were lower than usual (approximately 30%), the result of the poor solubility of ligand **3** in water. However, the resulting lanthanide complexes of **3** were found to be more soluble in water than the previously reported LnDOTA–$(BOM)_4$ complexes (where BOM is benzyloxymethyl ether) [20,21].

Binding studies with human serum albumin

Human serum albumin (HSA) is known to bind a variety of hydrophobic drugs in one of two major binding domains, referred to as site I and site II [22,23]. A variety of fluorescence methods have been developed to evaluate the binding sites and association constants of drugs with HSA. Site I is the primary binding site for drugs like warfarin and various phenylbutazone analogs, whereas diazepam and ibuprofen bind primarily at site II [24]. Warfarin itself has fluorescence properties (λ_{em} = 320 nm) that allow it to be used to assay binding at site I, whereas dansylsarcosine (λ_{em} = 360 nm) is frequently used as a fluorescent probe for site II [25]. Neither Gd**2** nor Gd**3** fluoresces at those wavelengths. Consequently, the ability of Gd**2** and Gd**3** to displace either of the fluorescent probes, warfarin or dansylsarcosine, from HSA was investigated by monitoring the changes in fluorescence with added Gd**2** or Gd**3**. Full details of this procedure have previously been reported by Caravan et al. [25]. The fluorescence emission intensity of these probes is higher when they are bound to HSA and consequently their emission intensity decreases when they are displaced from their normal binding sites by other compounds. The emission intensity of dansylsarcosine was found to fall after addition of either Gd**2** or Gd**3** to a solution containing an equal concentration of dansylsar-cosine (5 μM) and HSA (5 μM) at 298 K and pH 7.4 (Fig. 1). In contrast, little or no change in fluorescence intensity was observed when either Gd**2** or Gd**3** was added to a sample of HSA (5 μM) containing 1 equiv of warfarin (5 μM). This indicates that Gd**2** and Gd**3** both bind at a site II subdomain of HSA but have no, or only weak, binding affinity for site I. The data obtained for the displacement of dansylsarcosine from HSA by both Gd**2** and Gd**3** (Fig. 1) were fitted to an inhibition binding model (Eq. 2, Eq. 3).

$$[FP]_{bound} = \frac{A - \sqrt{A^2 - 4[HSA]_t[FP]_t}}{2} \quad (2)$$

where $A = [HSA]_t + [FP]_t + K_d^{app}$

$$K_d^{app} = \frac{1}{K_A}\left(1 + \frac{[GdL]_{free}}{K_I}\right) \quad (3)$$

Here $[FP]_{bound}$ and $[FP]_t$ are concentrations of the fluorescent probe bound to HSA and the total concentration of fluorescent probe, respectively, $[HSA]_t$ is the total concentration of HSA and $[GdL]_{free}$ is the concentration of unbound gadolinium complex. K_A is the association constant of the fluoresecent probe with HSA, K_d^{app} is the apparent dissociation constant of the fluorescent probe from HSA in the presence of Gd**2** and Gd**3**, and $1/K_I$ is the site-specific association constant of the gadolinium complexes with HSA. The value of K_A for HSA and dansylsarcosine in phosphate-buffered saline (PBS) (1.45×10^6 M^{-1}) was taken from the literature [26]. Fitting the titration curves obtained by displacement of dansylsarcosine with Gd**2** and Gd**3** (Fig. 1) to Eq. 2 and Eq. 3 gave $1/K_I$ values of 3.14 and 1.04×10^4 M^{-1} for the binding of Gd**2** and Gd**3** at site II, respectively. These association constants are considerably higher (40-fold) than those determined for the binding of GdEOB-DTPA is (where EOB-DTPA (2-ethoxybenzyl-diethylenetriamine pentaacetic acid) with HSA [16], a lipophilic hepatobiliary targeted CA, and are comparable with that of the high-affinity HSA binding blood pool agent MS-325 [25].

The binding of Gd**2** and Gd**3** to HSA was further verified by water proton relaxation titrations. The relaxivities of Gd**2** (1.9 mM^{-1} s^{-1}) and Gd**3** (2.2 mM^{-1} s^{-1}) (20 MHz, 298 K) resemble values reported for outer-sphere-only complexes (q = 0) [27] more closely than those of gadolinium complexes containing a single, inner-sphere coordinated water molecule (q = 1) [28]. However, these values are also consistent with complexes that have a single, inner-sphere water molecule that is in slow water exchange with bulk water (also validated in CEST spectra; see later). Upon addition of HSA, the relaxivities of Gd**2** and Gd**3** gradually increased with increasing HSA concentration to values approaching 4.6 and 5.9 mM^{-1} s^{-1} at 2 mM HSA, respectively, consistent with binding of the complexes to HSA (Fig. 2). This increase in relaxivity is small compared with that for other HSA-binding systems that exhibit more rapid water exchange [21,25,29], also indicating the water exchange kinetics in both Gd**2** and Gd**3** are slow.

CEST studies

PARACEST agents are commonly characterized by selectively presaturating an aqueous sample of the agent in incremental steps over a range of frequencies and plotting the remaining steady-state bulk water signal, M_S/M_0, versus saturation frequency. This was originally referred to as a Z-spectrum [30] and more recently as a CEST spectrum [31]. Figure 3 shows plots of M_S/M_0 versus saturation frequency for 40 mM Eu**2** and 20 mM Eu**3** both collected in pure water as solvent at 298 K. The peak at 0 ppm represents direct saturation of bulk water, while the peak centered near 54 ppm reflects the chemical exchange between a Eu^{3+}-bound water molecule and bulk solvent. The hyperfine shift and water exchange properties of EuDOTA tetraamide complexes typically have properties favorable for CEST with a peak arising from the slowly exchanging water molecule near 50 ppm. An approximately 35% decrease in bulk water signal intensity was observed for the Eu**3** sample, while the more highly concentrated Eu**2** sample resulted in a 64% decrease in bulk water signal intensity under identical conditions. Eu**2** proved to be more soluble in water (approximately 3 M) than Eu**3**.

In contrast to these EuDOTA tetraamide complexes, a water-exchange CEST peak is typically not seen for the corresponding Yb^{3+} complexes. This is believed to be the result of water exchange kinetics that lie outside the permissible range for CEST, viz., water exchange is too fast [32,33]. Nonetheless, a CEST effect arising from the amide protons of these ytterbium complexes can usually be observed [4,12] and so the CEST spectrum of Yb2 at 25 mM was recorded. Two different irradiation powers and durations were employed in the acquisition of these CEST spectra. Two peaks were detected near −18 and −56 ppm in the CEST spectrum when a relatively high-power (26-μT) presaturation pulse was applied for 1 s. These were assigned to the exchanging –NH amide protons in the complex; the peak at −18 ppm is at a shift similar to those reported for other Yb^{3+} complexes by Aime et al. [11] and Zhang et al. [12]. The peak at −56 ppm is unusually highly shifted; the largest shift previously reported was that observed by Aime et al. [13] and was −29 ppm. When a lower-power (6.5-μT) presaturation pulse was applied for 4 s, a broad (relatively fast exchanging) but detectable CEST peak was observed near 230 ppm. This peak can only be assigned to an exchanging inner-sphere water molecule on the Yb^{3+}. Although a Yb^{3+}-bound water resonance has not been detected previously by ^1H NMR, presumably owing to rapid water exchange, the chemical shift position for a Yb^{3+}-bound water molecule for ligand systems such as these was previously predicted to be near 200 ppm on the basis of chemical shift comparisons with other ligand resonances [32]. The low irradiation power and long duration used to record this spectrum were critical to the observation of this bound water molecule because at higher powers the rapid exchange kinetics and off-resonance direct saturation led to a coalescence of the bulk and bound water peaks, obscuring the CEST peak from the bound water. Although the CEST effect from the Yb^{3+}-bound water molecule in Yb**2** is relatively weak, this system does offer the possibility of using the CEST ratio (H_2O vs. NH) [10] as a direct indicator of sample pH (Fig. 4).

Many of the gadolinium complexes designed to bind to serum albumin have been reported to exhibit a change in their water exchange kinetics upon binding to the protein [17,25,34]. Usually the result is a deceleration of water exchange. Given the sensitivity of CEST to changes in water exchange rates [19,35] it is critical that binding of the PARACEST agents Ln**2** and Ln**3** to HSA does not result in adverse water exchange kinetics. Accordingly, the CEST spectra of Eu**2**, Yb**2**, Tm**2**, and Eu**3** were recorded in PBS (pH 7.4) in the presence and absence of HSA. The change in the CEST properties of the chelate upon binding to HSA were only minimal as exemplified by the spectra of Eu**2** with and without HSA (Fig. 5). The CEST spectra were recorded under conditions designed to ensure that essentially all of the Eu**2** was bound to HSA; the concentrations of both protein and PARACEST agent were 0.75 mM in a PBS buffer and for comparative purposes a second CEST spectrum was acquired in the absence of HSA. The two spectra resemble one another closely, although the width of the direct saturation peak at 0 ppm is greater in the presence of the protein, a result of proton-exchange events occurring between the protein and bulk water in addition to an increase in sample viscosity that shortens T_2. The similarity in the CEST peaks arising from the coordinated water molecule in the presence and absence of HSA indicates that the water exchange kinetics of the complex are not negatively impacted by the protein binding event. Color-coded CEST images of phantoms collected in the absence and presence of HSA (Fig. 6) demonstrate nicely that the images are relatively insensitive to the presence of protein.

The CEST spectra of Eu**2** shown in Fig. 5 were fitted to the Bloch equations modified for CEST [19]. This fitting procedure is hampered by the necessarily low concentration of PARACEST agent that results in small CEST effects, and the presence of the protein, which broadens the direct saturation peak. The latter is the most problematic during the fitting procedure because account must be taken for the additional OH, NH, and water molecules that are associated with the protein. The CEST spectrum of Eu**2** (Fig. 5, blue spectrum) was fitted to a two-pool (bulk and coordinated water) and three-pool (bulk and coordinated water and amide protons) model; the water residence lifetime (τ_M) obtained from this fitting was 1.0 ± 0.1 ms. This corresponds to a much slower rate of water exchange than was reported for the parent complex Eu**12** (τ_M = 0.38 ms), consistent with the hypothesis put forward by Aime et al. [36] that bulkier and more hydrophobic amide substituents lead to slower water exchange rates. In fitting the CEST spectrum of Eu**2** bound to HSA (Fig. 5, red spectrum) two approaches were taken. For model 1, no steps were taken to account for the presence of exchanging protons associated with the protein and allowed extremely short bulk water T_2 values to account for the increased linewidth of the bulk solvent. For model 2, a large number of exchanging protons that could exchange with bulk water but not the agent were added; the relaxation time, shift, and magnitude of this "protein" pool were allowed considerable freedom during the fitting procedure. The fitting of this spectrum is, as a result, highly qualitative; however, irrespective of the approach taken in fitting the data, the water residence lifetime (τ_M) of Eu**2** was found to decrease by a factor of approximately 2 upon binding to HSA. The water residence lifetime (τ_M) of Eu**2** bound to HSA was estimated at 0.44 ms from model 1 and 0.66 ms from model 2. This acceleration of the water exchange rate is in marked contrast to the deceleration in water exchange rate observed in many other systems [17,25,34] but is not without precedent; complexes entrapped in the protein apoferritin have been reported to undergo acceleration of water exchange [37,38].

Conclusions

Water exchange in Gd^{3+}-based CAs plays a part in determining the relaxation efficiency or relaxivity of a complex, particularly when the complex experiences slower rotation such as when it is bound to a macromolecule. The bound-water lifetime in octadentate complexes of Gd^{3+}, such as those formed with simple polyamino–polycarboxylate ligands like DTPA or DOTA, is typically 200–300 ns, but even this can limit the relaxivity of such complexes when they are targeted to a biological macromolecule. The optimal bound-water lifetime has been

estimated at 20–30 ns. CEST-based CAs are also sensitive to water exchange even in the absence of a macromolecular binding. If water exchange is too fast, the chemical shift of the exchanging water molecule averages with that of bulk water and CEST cannot be initiated, but if water exchange is too slow, the presaturated spins fully relax before CEST can occur. Hence, there is an optimal water exchange rate for any CEST agent and that optimal rate can be further influenced by the chemical environment of the agent. For example, acidic or basic environments have been shown to catalyze proton exchange between a slowly exchanging Ln^{3+}-bound water molecule and bulk water; this effect would be likely to alter the CEST properties of the agent [28], [41]. It has been reported that water exchange in Gd^{3+}-based CAs slows when such complexes are bound to albumin. For example, the bound-water lifetime in $GdDTPA(BOM)_3$, which also binds to HSA through benzyloxyether groups, increases by approximately 50% when this complex binds noncovalently to HSA [16]. The effect is even more dramatic in GdPCTP (where PCTP is 3,6,10,16-tetraazabicyclo[10.3.1]hexadeca-1(16), 12,14-triene-*N′*,*N″*,*N‴*-trimethylenephosphonic acid) [13], where the bound-water lifetime increases from approximately 8 to 290 ns (approximately 30-fold slower) when this $q = 1$ complex binds to HSA [40]. Such a substantial change in water exchange would have a profound influence on the CEST properties of similar albumin-binding PARACEST agents. In the case of Eu**2**, the bound-water lifetime determined from fitting CEST spectra indicates that water exchange accelerates (by a factor of approximately 2) when this complex binds with HSA. Given the slow water exchange rate in this complex when it is not bound to HSA, the change in water exchange rate was found to have little influence on the CEST properties of the agent upon binding to HSA. The slow water exchange kinetics of these complexes mean that a CEST effect arising from the protons of a water molecule coordinated to Yb^{3+} can be observed for the first time.

In summary, fluorescence displacement experiments showed that both Gd**2** and Gd**3** bind reversibly at site II of HSA and this results in a slowing of water exchange by about two fold. The relatively small increase in water proton relaxivity that was observed upon addition of HSA to either Gd**2** or Gd**3** is also consistent with slow water exchange systems both in the absence and in the presence of HSA. The fact that HSA has a high binding affinity for these PARACEST agents and that CEST is not quenched by protein binding make them potentially useful as vasculature imaging agents although improvements in sensitivity may be required prior to in vivo application.

Acknowledgements

This research was supported in part by grants from the National Institutes of Health (CA-115531, DK-058398, EB-04285, and RR-02584), the Department of Defense Breast Cancer Research Program (Idea grant W81XWH-05-1-0223), and the Robert A. Welch Foundation (AT-584).

References

1. Merbach, AE.; Toth, E. The chemistry of contrast agents in medical magnetic resonance imaging. Chichester: Wiley; 2001.
2. Caravan P, Ellison JJ, McMurry TJ, Lauffer RB. Chem Rev 1999;99:2293–2352. [PubMed: 11749483]
3. Ward KM, Balaban RS. Magn Reson Med 2000;44:799–802. [PubMed: 11064415]
4. Terreno E, Castelli Daniela D, Cravotto G, Milone L, Aime S. Invest Radiol 2004;39:235–243. [PubMed: 15021328]
5. Goffeney N, Bulte JWM, Duyn J, Bryant LH Jr, van Zijl PCM. J Am Chem Soc 2001;123:8628–8629. [PubMed: 11525684]
6. Snoussi K, Bulte JWM, Gueron M, van Zijl PCM. Magn Reson Med 2003;49:998–1005. [PubMed: 12768576]

7. Zhou J, Payen J-F, Wilson DA, Traystman RJ, van Zijl PCM. Nat Med 2003;9:1085–1090. [PubMed: 12872167]
8. Zhang S, Winter P, Wu K, Sherry AD. J Am Chem Soc 2001;123:1517–1518. [PubMed: 11456734]
9. Zhang S, Wu K, Sherry AD. J Am Chem Soc 2002;124:4226–4227. [PubMed: 11960448]
10. Aime S, Barge A, Castelli DD, Fedeli F, Mortillaro A, Nielsen FU, Terreno E. Magn Reson Med 2002;47:639–648. [PubMed: 11948724]
11. Aime S, Castelli DD, Terreno E. Angew Chem Int Ed Engl 2002;41:4334–4336. [PubMed: 12434381]
12. Zhang S, Michaudet L, Burgess S, Sherry AD. Angew Chem Int Ed Engl 2002;41:1919–1921. [PubMed: 19750633]
13. Aime S, Delli Castelli D, Fedeli F, Terreno E. J Am Chem Soc 2002;124:9364–9365. [PubMed: 12167018]
14. Zhang S, Trokowski R, Sherry AD. J Am Chem Soc 2003;125:15288–15289. [PubMed: 14664562]
15. Zhang S, Malloy C, Sherry AD. J Am Chem Soc 2005;127:17572–17573. [PubMed: 16351064]
16. Aime S, Chiaussa M, Digilio G, Gianolio E, Terreno E. J Biol Inorg Chem 1999;4:766–774. [PubMed: 10631608]
17. Aime S, Botta M, Fasano M, Crich SG, Terreno E. J Biol Inorg Chem 1996;1:312–319.
18. Kovacs Z, Sherry AD. J Chem Soc Chem Commun 1995:185–186.
19. Woessner DE, Zhang S, Merritt ME, Sherry AD. Magn Reson Med 2005;53:790–799. [PubMed: 15799055]
20. Aime S, Botta M, Ermondi G, Fedeli F, Uggeri F. Inorg Chem 1992;31:1100–1103.
21. Hovland R, Aasen AJ, Klaveness J. Org Biomol Chem 2003;1:1707–1710. [PubMed: 12926358]
22. Sudlow G, Birkett DJ, Wade DN. Mol Pharm 1976;12:1052–1061.
23. Sudlow G, Birkett DJ, Wade DN. Mol Pharm 1975;11:824–832.
24. Peters, TJ. All about albumin: biochemistry, genetics and medicinal applications. San Diego: Academic; 1996.
25. Caravan P, Cloutier NJ, Greenfield MT, McDermid SA, Dunham SU, Bulte JWM, Amedio JC Jr, Looby RJ, Supkowski RM, Horrocks WD Jr, McMurry TJ, Lauffer RB. J Am Chem Soc 2002;124:3152–3162. [PubMed: 11902904]
26. Sakai T, Yamasaki K, Sako T, Kragh-Hansen U, Suenaga A, Otagiri M. Pharm Res 2001;18:520–524. [PubMed: 11451040]
27. Geraldes CFGC, Urbano AM, Alpoim MC, Sherry AD, Kuan KT, Rajagopalan R, Maton F, Muller RN. Magn Reson Imaging 1995;13:401–420. [PubMed: 7791550]
28. Aime S, Barge A, Bruce JI, Botta M, Howard JAK, Moloney JM, Parker D, de Sousa AS, Woods M. J Am Chem Soc 1999;121:5762–5771.
29. Woods M, Zhang S, Von Howard E, Sherry AD. Chem Eur J 2003;9:4634–4640.
30. Grad J, Bryant RG. J Magn Reson 1990;90:1–8.
31. Ward KM, Aletras AH, Balaban RS. J Magn Reson 2000;143:79–87. [PubMed: 10698648]
32. Zhang S, Sherry AD. J Solid State Chem 2003;171:38–43.
33. Zhang S, Merritt M, Woessner DE, Lenkinski RE, Sherry AD. Acc Chem Res 2003;36:783–790. [PubMed: 14567712]
34. Aime S, Gianolio E, Longo D, Pagliarin R, Lovazzano C, Sisti M. Chem Biol Chem 2005;6:818–820.
35. Woods M, Woessner DE, Sherry AD. Chem Soc Rev 2006;35:500–511. [PubMed: 16729144]
36. Aime S, Barge A, Batsanov AS, Botta M, Castelli DD, Fedeli F, Mortillaro A, Parker D, Puschmann H. Chem Commun 2002:1120–1121.
37. Aime S, Frullano L, Geninatti Crich S. Angew Chem Int Ed Engl 2002;41:1017–1019. [PubMed: 12491298]
38. Vasalatiy O, Zhao P, Zhang S, Aime S, Sherry AD. Contrast Media Mol Imaging 2006;1:10–14. [PubMed: 17193595]
40. Aime S, Botta M, Crich SG, Giovenzana GB, Pagliarin R, Piccinini M, Sisti M, Terreno E. J Biol Inorg Chem 1997;2:470–479.

41. Kálmán FK, Woods M, Caravan P, Jurek P, Spiller M, Tircsó G, Király R, Brücher R, Sherry AD. Inorg Chem. 2007

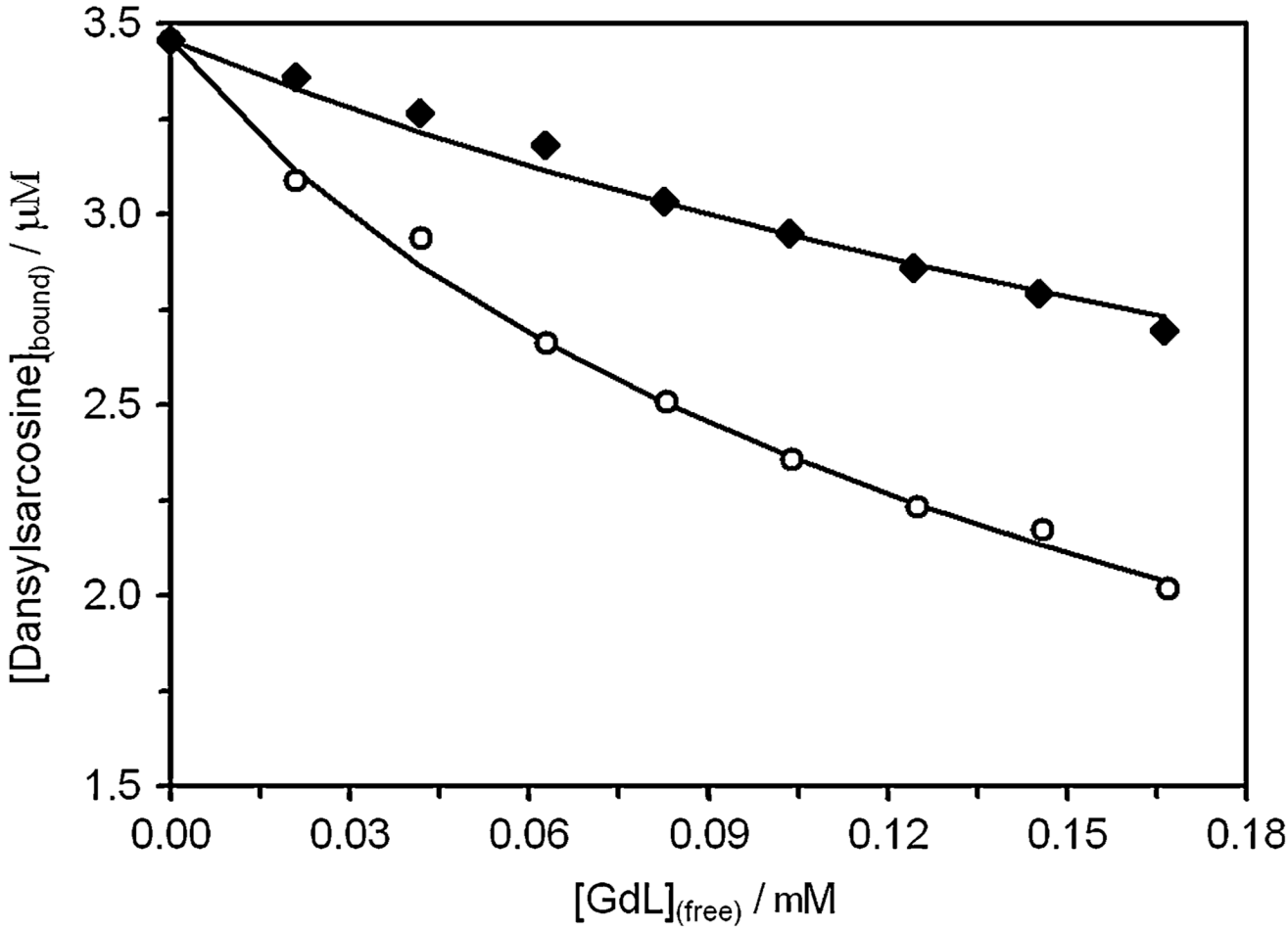

Fig. 1.
The inhibition of dansylsarcosine binding to human serum albumin (HSA) by Gd**2** (*circles*) and Gd**3** (*diamonds*)

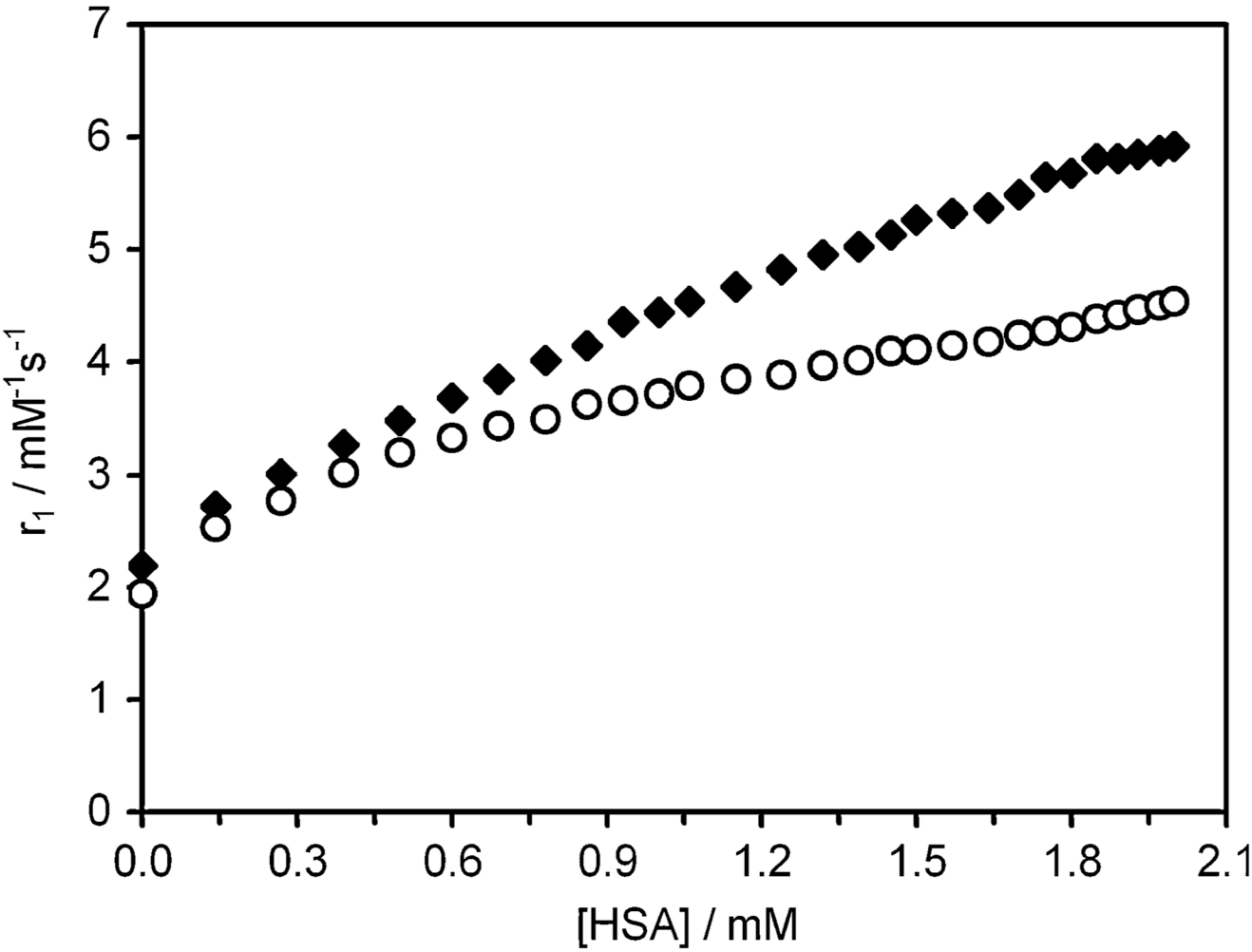

Fig. 2.

Binding of the complexes Gd**2** (*circles*) and Gd**3** (*diamonds*) to HSA has the effect of increasing the longitudinal relaxivity (r_1) of each complex. Titrations were performed at 20 MHz, 298 K, in *N*-(2-hydroxyethyl)piperazine-N′-ethanesulfonic acid buffer, pH 7.4

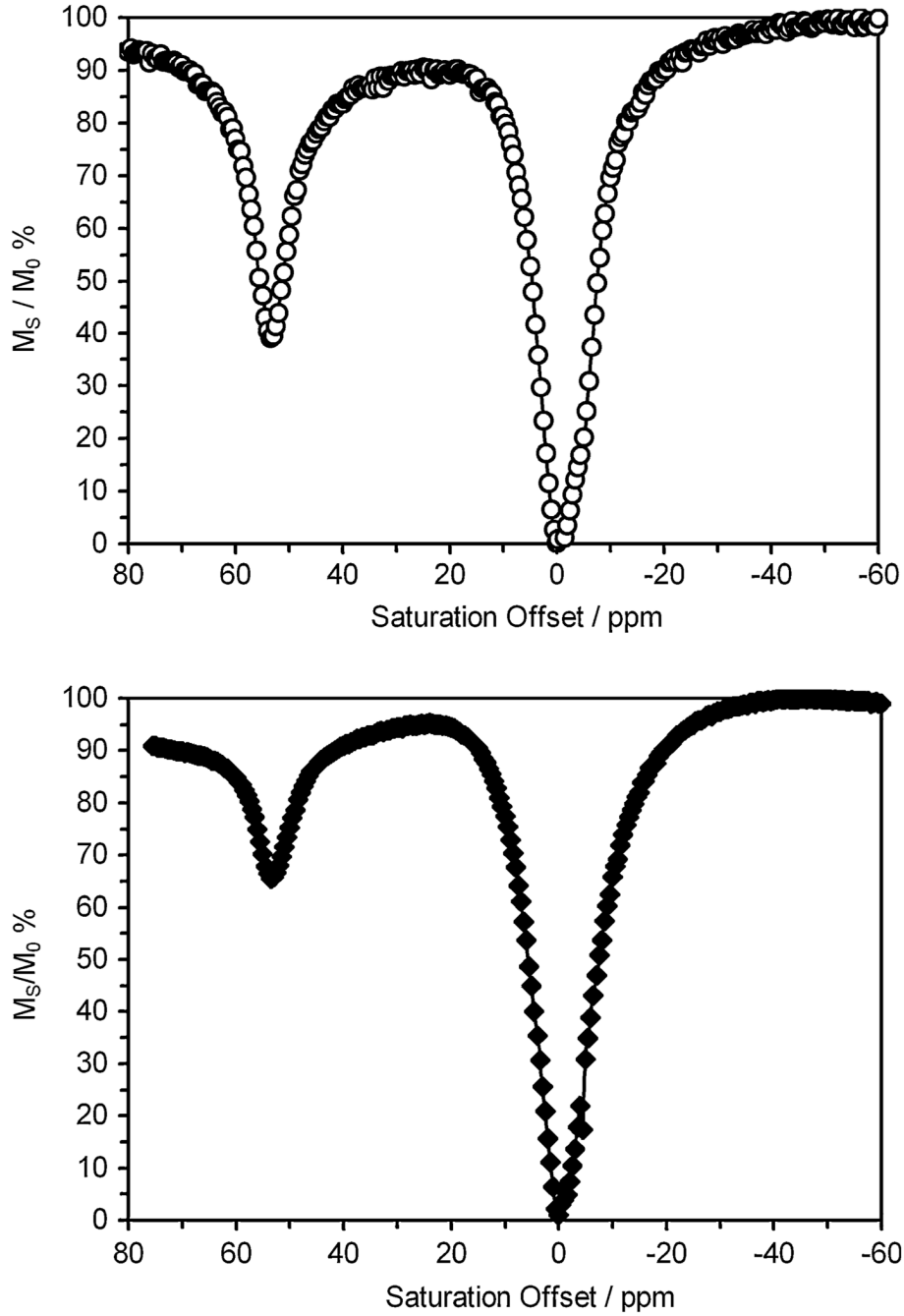

Fig. 3.

Chemical exchange saturation transfer (CEST) spectra, plotting the solvent water signal intensity (expressed as a percentage of its initial intensity) against presaturation frequency, for a 40 mM aqueous solution of Eu**2** (*top*) and a 20 mM aqueous solution of Eu**3** (*bottom*) at 298 K, irradiation time 2 s, B_1 = 26 μT

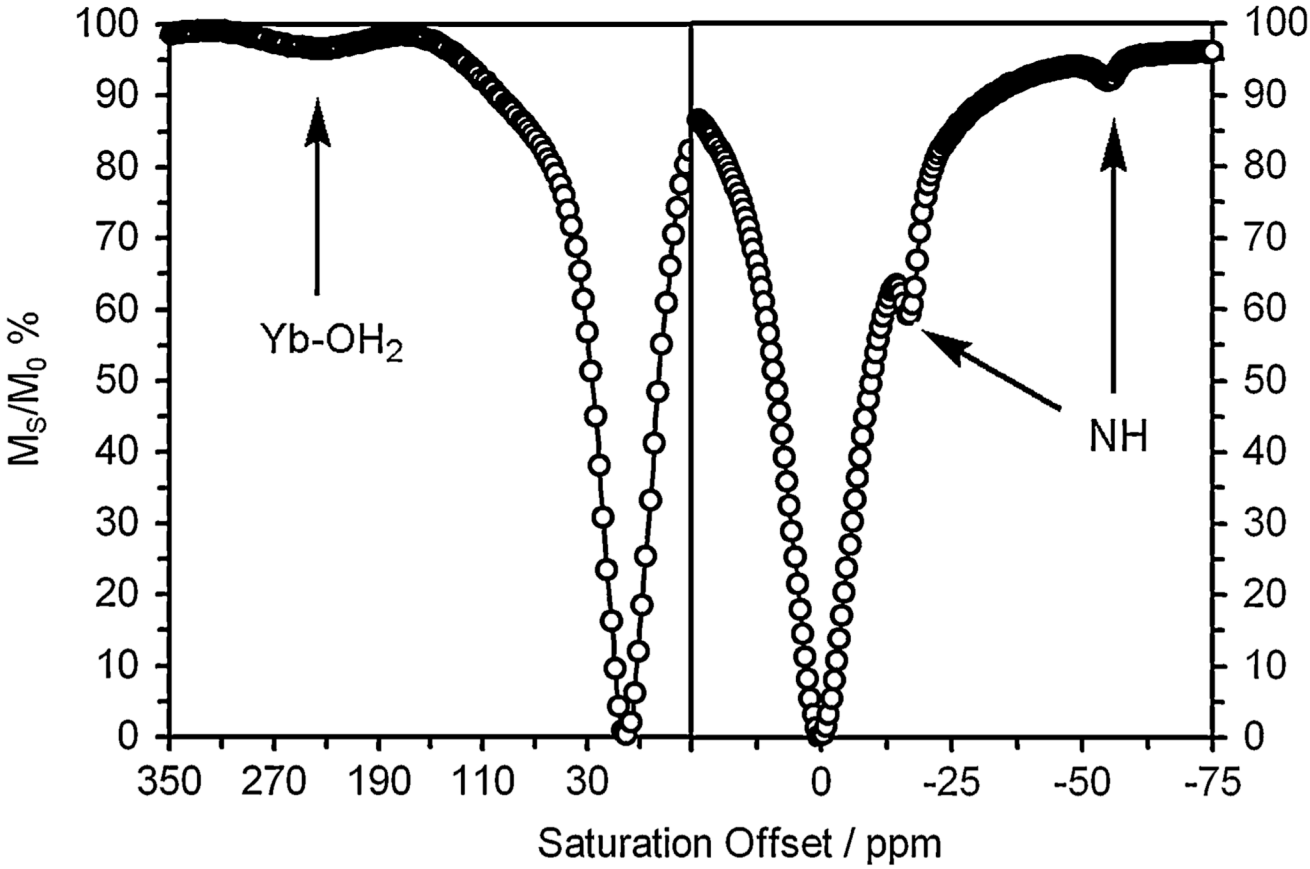

Fig. 4.

CEST spectra of a 25 mM solution of Yb**2** recorded at 500 MHz, pH 7.4, and 298 K. On the *left* is shown the downfield region of the spectrum recorded with an irradiation time of 4 s, $\boldsymbol{B}_1$ = 6.5 μT; a small CEST peak arising from the coordinated water molecule is clearly visible. On the *right* is shown the upfield region for an irradiation time of 1 s, $\boldsymbol{B}_1$ = 26 μT; CEST peaks arising from the amide NH protons can be seen

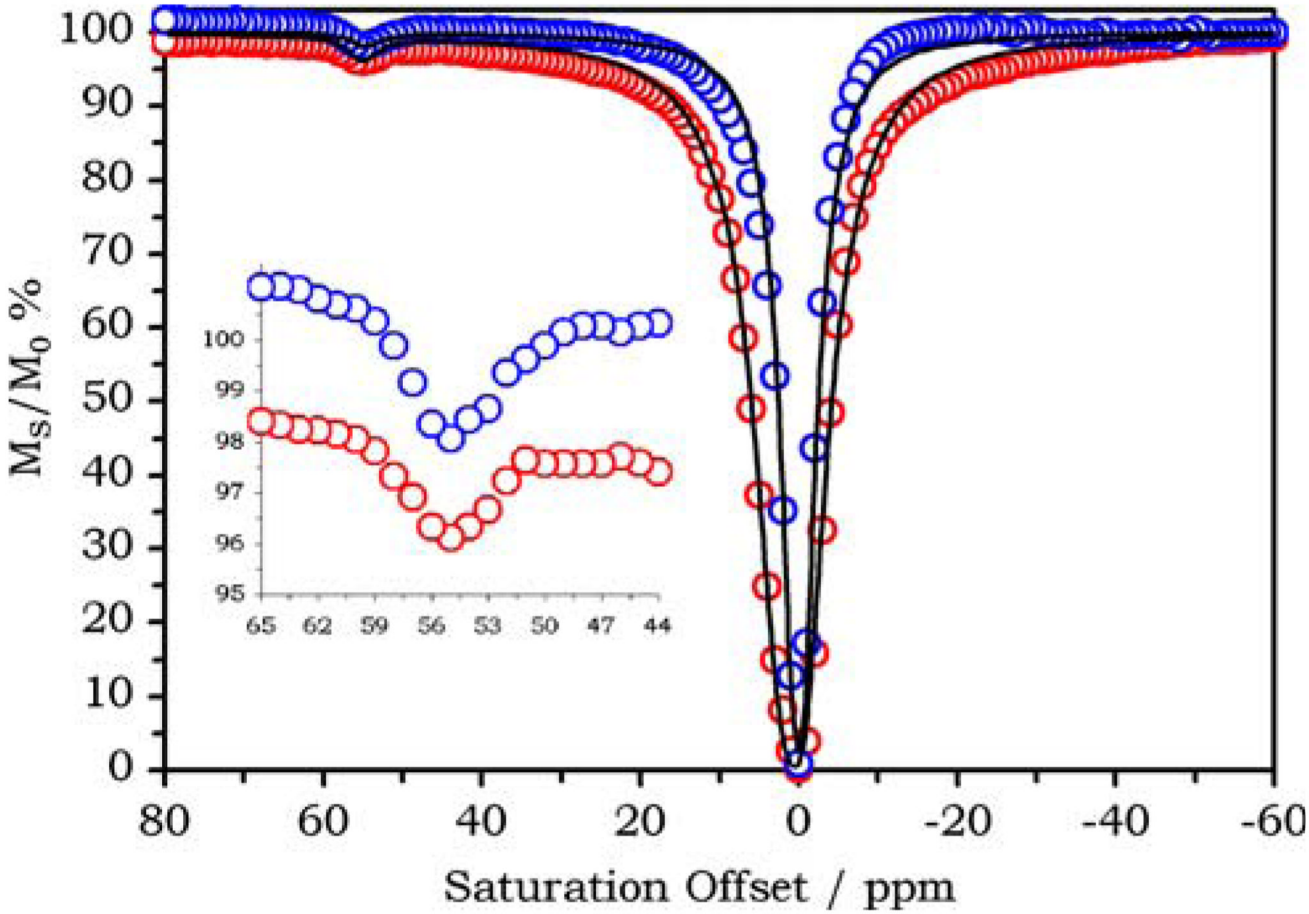

Fig. 5.

The CEST spectra of 0.75 mM Eu**2** in phosphate-buffered saline (PBS) recorded in the absence (*blue*) and presence (*red*) of 0.75 mM HSA. $\boldsymbol{B}_0$ = 400 MHz, $\boldsymbol{B}_1$ = 19 μT, irradiation time 6 s, 298 K

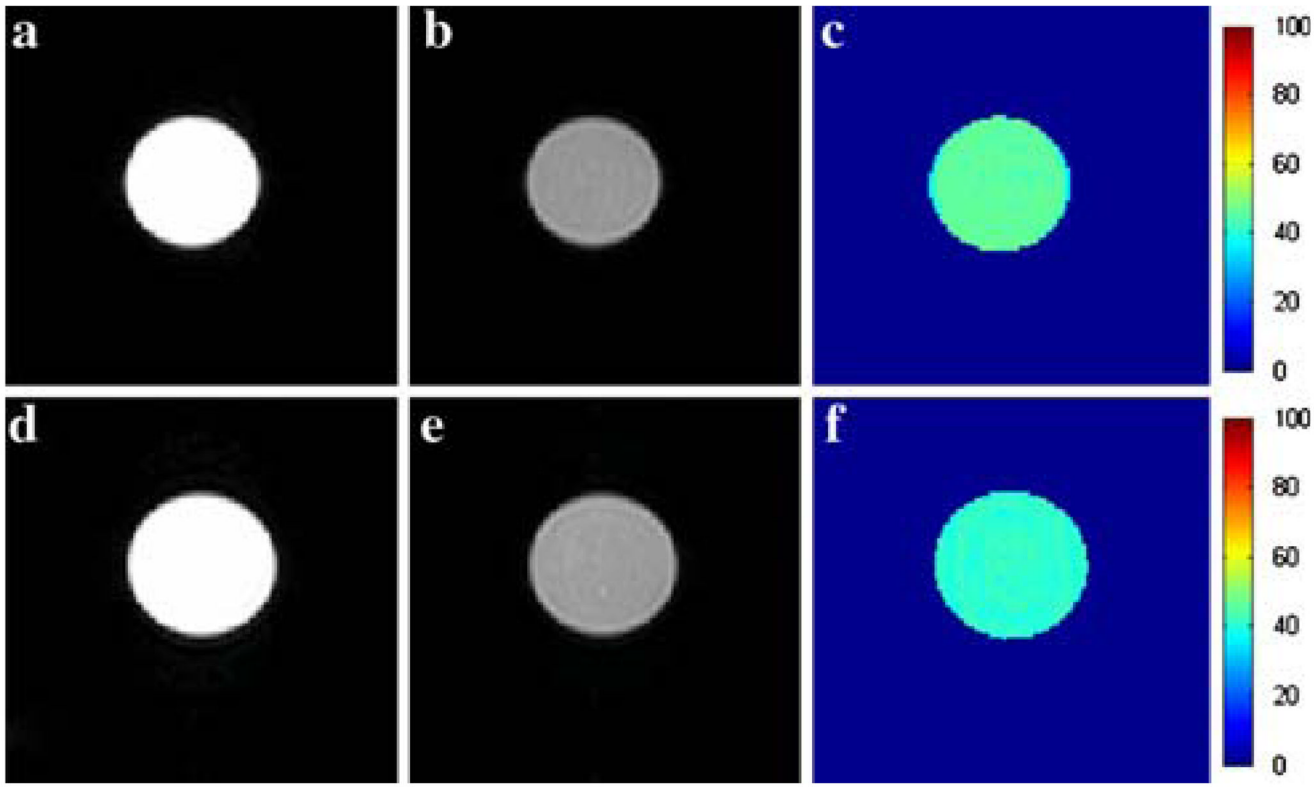

Fig. 6.

Images of 20 mM solutions of Eu**2** in the absence and presence of 5% HSA. *Left* (*a*, *d*), *center* (*b*, *e*), and *right* (*c*, *f*) columns represent the off-resonance (−54 ppm), on-resonance (54 ppm), and the percentage CEST enhancement maps, respectively. Samples in the *top row* contained 20 mM Eu**2** in PBS, while samples in the *bottom row* contained in addition 5% HSA (Buminate®). Each image was collected using a standard spin-echo sequence with a 6-s presaturation pulse applied at the indicated offset

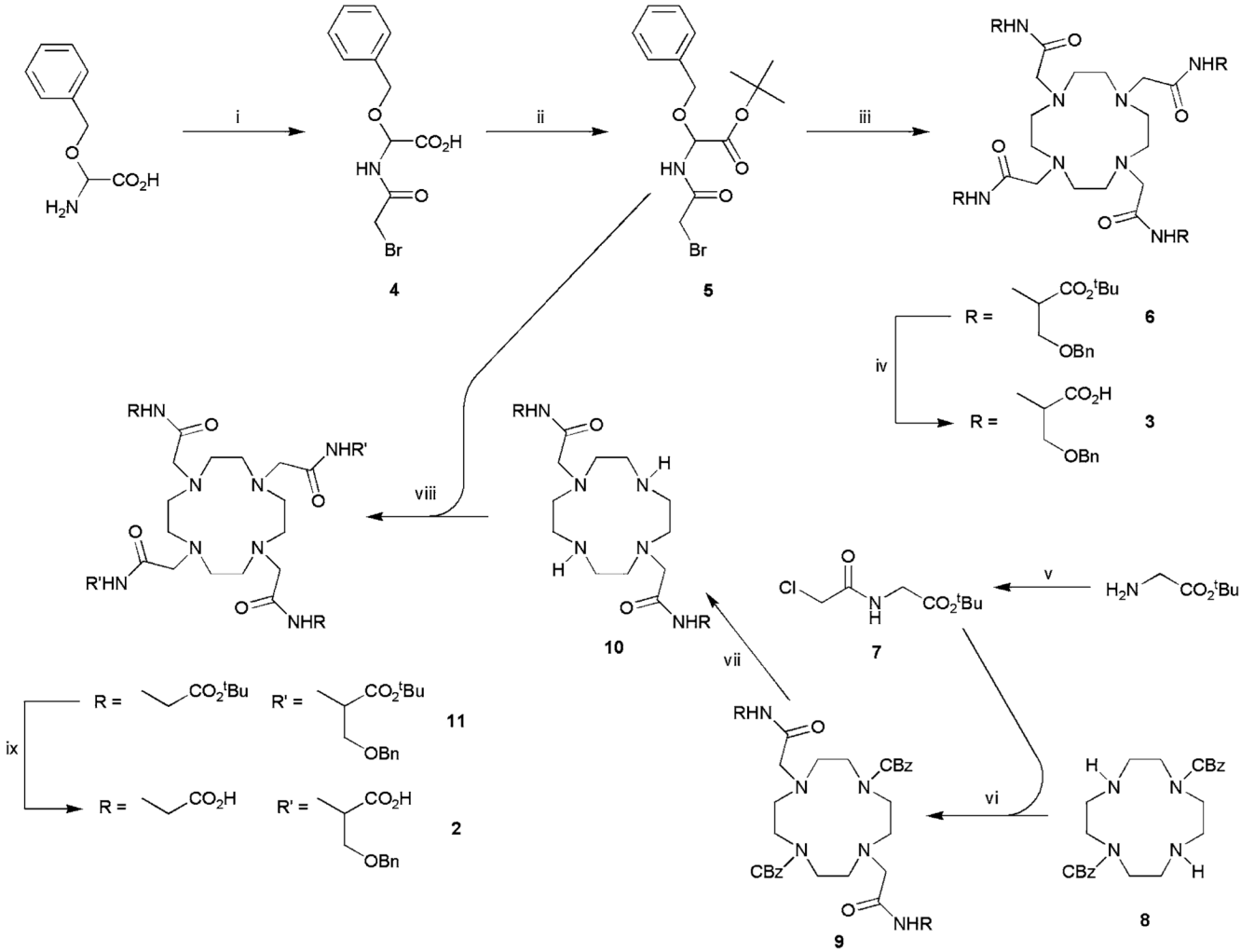

Scheme 1.

The synthetic route to ligands **2** and **3**. Reagents and conditions: *i* $BrCH_2COBr/K_2CO_3/NaOH/273$ K; *ii tert*-butyl trichloroacetimidate/BF_3·OEt/tetrahydrofuran/273 K; *iii* cyclen/$^{i}Pr_2NEt$/MeCN/328 K; *iv* trifluoroacetic acid (TFA); *v* $ClCH_2COCl/K_2CO_3/H_2O/CH_2Cl_2/273$ K; *vi* K_2CO_3/MeCN/333 K; *vii* H_2/Pd on C; *viii* $^{i}Pr_2NEt$/MeCN/333 K; *ix* TFA

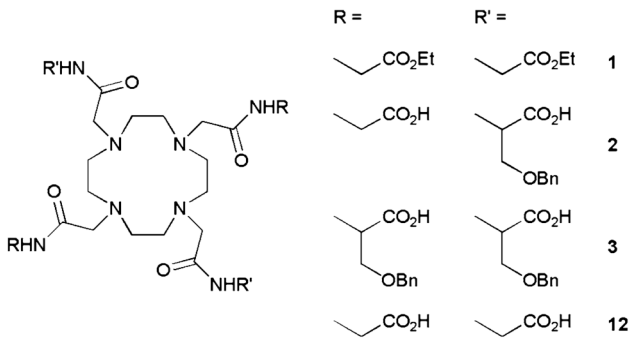

Structure 1.